These notes are from the draft CRISTAL User's Guide for remote sensing of water IOPs, bottom depth, and bottom type with hyperspectral imagery. CRISTAL is Comprehensive Reflectance Inversion based on Spectrum matching and TAble Lookup.

Curtis Mobley **May 2011**

Appendix A.
Comparison of Terrestrial and Shallow-water Remote Sensing: Thematic Mapping Techniques vs. CRISTAL

A.1. Background

As noted in Section 1.5, the simultaneous retrieval of bathymetry, bottom classification, and water IOPs is a much more difficult task than thematic mapping to determine land surface type, as used in terrestrial remote sensing. In terrestrial thematic mapping, only the type of land surface must be deduced from an atmospherically corrected image spectrum; there are no confounding influences by water IOPs and depth.

In supervised classification the object is to associate a given image spectrum with one of several pre-determined classes of spectra. In terrestrial remote sensing these classes are typically defined as soil, grass, trees, water, pavement, etc. A thematic map of earth surface features is then generated by classifying the spectrum from each image pixel into one of the pre-determined classes.

One approach to supervised classification is to compute the mean spectrum for each class and a corresponding covariance matrix that defines the "size" of each class of spectra about its mean. The image spectrum is then compared only with the mean spectrum and "size" for each class, and the image spectrum is statistically associated with the class it is most likely to belong to according to some metric for distance between the image a mean spectra and user-specified assumptions about the statistical properties of the class members.

This appendix considers the terrestrial and oceanic problems in more detail and shows that the standard terrestrial thematic mapping methodologies are not easily applied to the ocean remote sensing problem addressed by CRISTAL.

A. 2. Covariance and Correlation Matrices

Consider a collection of N remote sensing reflectance spectra R_{rs}, each with K wavelengths, which we denote by $R_n(\lambda_k)$, $n = 1,...,N$ and $k=1,...,K$ (dropping the "rs" subscript on R_{rs} for convenience). The spectra can be regarded as column vectors:

$$\boldsymbol{R}_n = \begin{bmatrix} R_n(\lambda_1) \\ R_n(\lambda_2) \\ \vdots \\ R_n(\lambda_K) \end{bmatrix} = \left[R_n(\lambda_1),\ R_n(\lambda_2),\ \cdots,\ R_n(\lambda_K) \right]^{\mathrm{T}},$$

where bold type indicates a vector or matrix, and superscript T indicates transpose. In CRISTAL, these spectra are the CRISTAL database spectra, N is usually 10^5 or more, and K is 75 for spectra from 380 to 750 nm with 5 nm resolution. Let $\boldsymbol{I} = [R(\lambda_1), R(\lambda_2), ..., R(\lambda_K)]^{\mathrm{T}}$ be the image spectrum that is to be classified.

Now consider subsets of the entire CRISTAL database that define various classes of spectra. To be specific in the illustrative computations below, we chose four classes of spectra: R_{rs} for 10 sand and sediment spectra seen through 0.01 m of water (having IOPs typical of the Bahamas), 10 coral spectra seen through 0.01 m of water, and the same sand and coral spectra seen through 10 m of the same water. Figure A.1 shows the individual spectra in these four classes. To minimize the array sizes for the printout of Table A.1 below, we subsampled the spectra to wavelengths of 400, 450, ..., 650, 700 nm, so that $K = 7$. The subsampled spectra are shown in Fig. A.2.

These spectra are obviously correlated in wavelength. The amount of correlation between one wavelength and another is quantified by the covariance and correlation matrices, which are computed as follows. Let $m = 1,..., M$ label the class, with M being the total number of classes (here 4). Class m contains N_m spectra (here, $N_m = 10$ for each class). Then the mean or average spectrum for each class is defined by

$$\bar{R}_m(\lambda_i) = \frac{1}{N_m} \sum_{n=1}^{N_m} R_n(\lambda_i),$$

where the sum is over the spectra belonging to class m. In vector notation this is

$$\bar{\boldsymbol{R}}_m = \frac{1}{N_m} \sum_{n=1}^{N_m} \boldsymbol{R}_n .$$

The mean spectra for the example four classes are shown by the heavy lines in Fig. A.2.

The elements of the $K \times K$ class covariance matrices $\boldsymbol{\Sigma}_m$ are defined by

$$\Sigma_m(i,j) = \frac{1}{N_m - 1} \sum_{n=1}^{N_m} \left[R_n(\lambda_i) - \bar{R}_m(\lambda_i) \right] \left[R_n(\lambda_j) - \bar{R}_m(\lambda_j) \right] .$$

$\Sigma_m(i,j)$ expresses the covariance of the class spectra at wavelength λ_i with λ_j; $\Sigma_m(i,i)$ is the variance

of the class spectra at λ_i. For remote-sensing reflectance spectra R_{rs} with units of sr^{-1}, the units of $\Sigma_m(i,j)$ are sr^{-2}. If we arrange the spectrum column vectors for class m in a $K \times N_m$ matrix with the class mean removed,

$$\boldsymbol{R}_{(m)} = \begin{bmatrix} R_1(\lambda_1) - \bar{R}_m(\lambda_1) & \cdots & R_{N_m}(\lambda_1) - \bar{R}_m(\lambda_1) \\ \vdots & \vdots & \vdots \\ R_1(\lambda_K) - \bar{R}_m(\lambda_K) & \cdots & R_{N_m}(\lambda_1) - \bar{R}_m(\lambda_K) \end{bmatrix},$$

then the covariance matrix for class m can be compactly written as

$$\boldsymbol{\Sigma}_m = \frac{1}{N_m - 1} \boldsymbol{R}_{(m)} \boldsymbol{R}_{(m)}^T .$$

The elements of the $K \times K$ correlation matrix $\boldsymbol{\rho}_m$ for class m are defined from the class covariance matrix $\boldsymbol{\Sigma}_m$ by

$$\rho_m(i,j) = \frac{\Sigma_m(i,j)}{\sqrt{\Sigma_m(i,i)\ \Sigma_m(j,j)}} .$$

Table A.1 shows the class covariance and correlation matrices computed by these equations for the four classes of spectra shown in Fig. A.2. These specific examples make it clear that

- R_{rs} at one wavelength is highly correlated with R_{rs} at another wavelength, as expected.

- The covariance and correlation matrices are different for each class. Thus these matrices depend not only on bottom type (sand vs coral) but also on bottom depth (and water IOPs, not explicitly shown here). In other words, *the wavelength covariances carry information about both bottom type and water depth and IOPs*.

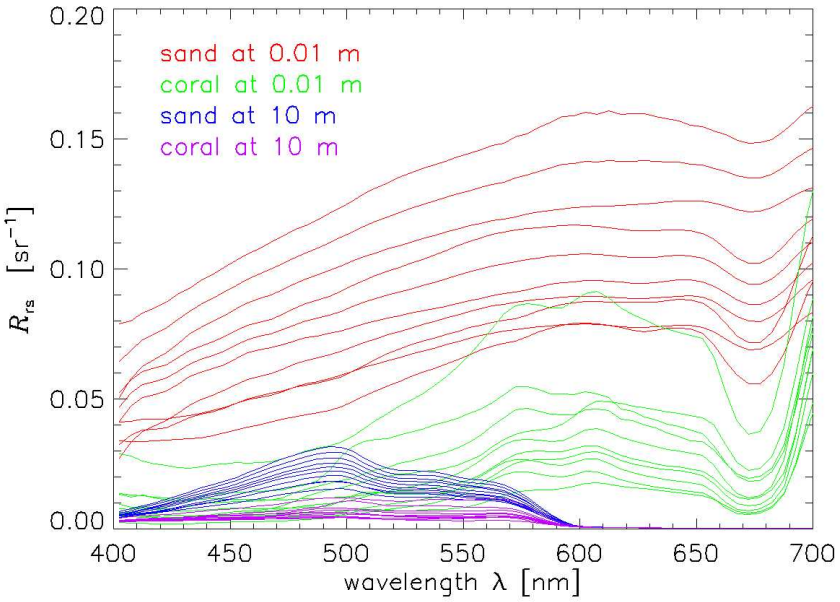

Fig. A.1. CRISTAL database R_{rs} spectra defining the four classes; each class has 10 spectra.

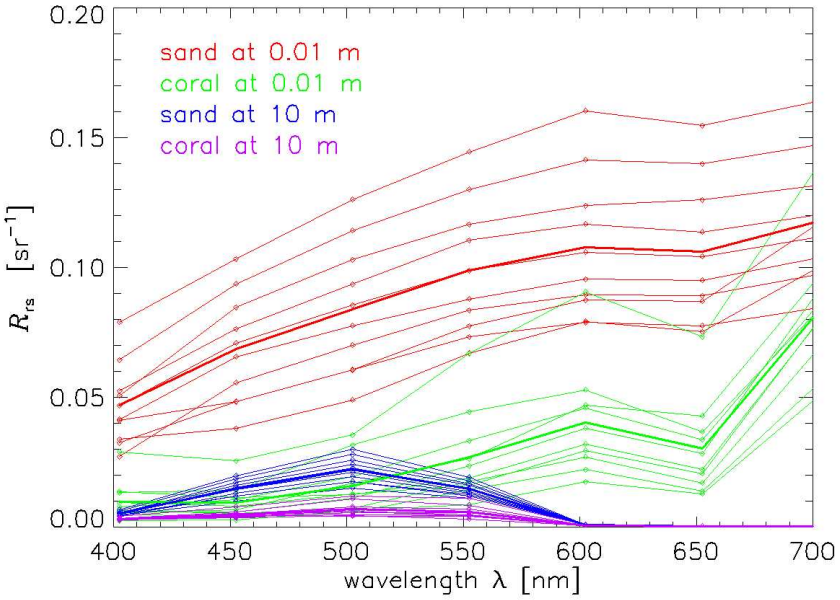

Fig. A.2. The spectra of Fig. A.1 as resampled at 50 nm intervals for use in the illustrative computations (light lines). The heavy lines are the class mean spectra.

Table A.1. Covariance and correlation matrices for the four classes of spectra seen in Fig. A.2. Wavelength 1 (400 nm) is at the upper left and wavelength 7 (700 nm) is at the lower right of each array. Units for $\mathbf{\Sigma}$ are sr^{-2}; $\boldsymbol{\rho}$ is non-dimensional.

Covariance matrix Σ for sand at 0.01 m:

2.462e-004	3.049e-004	3.612e-004	3.797e-004	4.141e-004	3.994e-004	3.625e-004
3.049e-004	4.547e-004	5.361e-004	5.447e-004	5.712e-004	5.639e-004	4.569e-004
3.612e-004	5.361e-004	6.338e-004	6.462e-004	6.787e-004	6.692e-004	5.449e-004
3.797e-004	5.447e-004	6.462e-004	6.658e-004	7.046e-004	6.912e-004	5.780e-004
4.141e-004	5.712e-004	6.787e-004	7.046e-004	7.546e-004	7.364e-004	6.340e-004
3.994e-004	5.639e-004	6.692e-004	6.912e-004	7.364e-004	7.230e-004	6.179e-004
3.625e-004	4.569e-004	5.449e-004	5.780e-004	6.340e-004	6.179e-004	5.856e-004

Correlation matrix ρ for sand at 0.01 m:

1.000	0.911	0.914	0.938	0.961	0.947	0.955
0.911	1.000	0.999	0.990	0.975	0.983	0.885
0.914	0.999	1.000	0.995	0.981	0.989	0.894
0.938	0.990	0.995	1.000	0.994	0.996	0.926
0.961	0.975	0.981	0.994	1.000	0.997	0.954
0.947	0.983	0.989	0.996	0.997	1.000	0.950
0.955	0.885	0.894	0.926	0.954	0.950	1.000

Covariance matrix Σ for coral at 0.01 m:

5.793e-005	4.952e-005	6.378e-005	1.143e-004	1.389e-004	1.129e-004	1.552e-004
4.952e-005	4.442e-005	6.222e-005	1.080e-004	1.299e-004	1.059e-004	1.417e-004
6.378e-005	6.222e-005	1.070e-004	1.712e-004	2.007e-004	1.655e-004	2.057e-004
1.143e-004	1.080e-004	1.712e-004	3.010e-004	3.578e-004	2.961e-004	3.775e-004
1.389e-004	1.299e-004	2.007e-004	3.578e-004	4.432e-004	3.774e-004	4.950e-004
1.129e-004	1.059e-004	1.655e-004	2.961e-004	3.774e-004	3.300e-004	4.306e-004
1.552e-004	1.417e-004	2.057e-004	3.775e-004	4.950e-004	4.306e-004	6.132e-004

Correlation matrix ρ for coral at 0.01 m:

1.000	0.976	0.810	0.865	0.867	0.817	0.823
0.976	1.000	0.903	0.934	0.926	0.875	0.859
0.810	0.903	1.000	0.954	0.922	0.881	0.803
0.865	0.934	0.954	1.000	0.980	0.940	0.879
0.867	0.926	0.922	0.980	1.000	0.987	0.949
0.817	0.875	0.881	0.940	0.987	1.000	0.957
0.823	0.859	0.803	0.879	0.949	0.957	1.000

Covariance matrix Σ for sand at 10 m:

5.792e-007	2.174e-006	3.341e-006	1.880e-006	4.235e-008	2.783e-009	2.886e-012
2.174e-006	1.006e-005	1.542e-005	8.357e-006	1.805e-007	1.214e-008	1.047e-011
3.341e-006	1.542e-005	2.369e-005	1.288e-005	2.785e-007	1.872e-008	1.645e-011
1.880e-006	8.357e-006	1.288e-005	7.086e-006	1.545e-007	1.033e-008	9.641e-012
4.235e-008	1.805e-007	2.785e-007	1.545e-007	3.409e-009	2.267e-010	2.151e-013
2.783e-009	1.214e-008	1.872e-008	1.033e-008	2.267e-010	1.517e-011	1.457e-014
2.886e-012	1.047e-011	1.645e-011	9.641e-012	2.151e-013	1.457e-014	2.776e-017

Correlation matrix ρ for sand at 10 m:

1.000	0.900	0.902	0.928	0.953	0.939	0.720
0.900	1.000	0.999	0.990	0.975	0.983	0.626
0.902	0.999	1.000	0.994	0.980	0.987	0.641
0.928	0.990	0.994	1.000	0.994	0.996	0.687
0.953	0.975	0.980	0.994	1.000	0.997	0.699
0.939	0.983	0.987	0.996	0.997	1.000	0.710
0.720	0.626	0.641	0.687	0.699	0.710	1.000

Covariance matrix Σ for coral at 10 m:

1.956e-007	5.520e-007	9.484e-007	9.105e-007	2.255e-008	1.305e-009	1.714e-012
5.520e-007	1.638e-006	3.068e-006	2.868e-006	7.055e-008	4.100e-009	4.858e-012
9.484e-007	3.068e-006	7.054e-006	6.135e-006	1.484e-007	8.731e-009	8.282e-012
9.105e-007	2.868e-006	6.135e-006	5.845e-006	1.424e-007	8.393e-009	9.001e-012
2.255e-008	7.055e-008	1.484e-007	1.424e-007	3.620e-009	2.197e-010	2.322e-013
1.305e-009	4.100e-009	8.731e-009	8.393e-009	2.197e-010	1.372e-011	1.359e-014
1.714e-012	4.858e-012	8.282e-012	9.001e-012	2.322e-013	1.359e-014	2.221e-017

Correlation matrix ρ for coral at 10 m:

1.000	0.975	0.807	0.852	0.847	0.797	0.823
0.975	1.000	0.903	0.927	0.916	0.865	0.805
0.807	0.903	1.000	0.955	0.928	0.888	0.662
0.852	0.927	0.955	1.000	0.979	0.937	0.790
0.847	0.916	0.928	0.979	1.000	0.986	0.819
0.797	0.865	0.888	0.937	0.986	1.000	0.778
0.823	0.805	0.662	0.790	0.819	0.778	1.000

A.3. CRISTAL Classification vs. Statistical Classification

One spectrum-matching option in CRISTAL uses a simple Euclidean metric to measure the squared distance (in units of sr^{-2}) between an image spectrum $\boldsymbol{I}$ and each $\boldsymbol{R}_n$ in the CRISTAL database:

$$D_E^2(n) = \sum_{i=1}^{K} [R_n(\lambda_i) - I(\lambda_i)]^2 = [\boldsymbol{R}_n - \boldsymbol{I}]^T [\boldsymbol{R}_n - \boldsymbol{I}] .$$

The spectrum $\boldsymbol{R}_n$ giving the minimum distance $D_E^2(n)$ of all N database spectra determines the closest match to the image spectrum $\boldsymbol{I}$. Note that this is not a statistical estimate in the sense that no probability model is involved. Note also that the image spectrum is being compared with every spectrum in the CRISTAL database, not just with pre-defined class mean spectra.

In traditional thematic classification, an image spectrum $\boldsymbol{I}$ is compared only with the mean spectrum and "size" for each class, as expressed by the class mean $\bar{\boldsymbol{R}}_m$ and covariance $\boldsymbol{\Sigma}_m$. Here we use "size" in the sense that the variances and covariances in $\boldsymbol{\Sigma}_m$ are larger when the spread of R_{rs} spectra is greater. Inspect, for example, the elements of $\boldsymbol{\Sigma}_m$ for the class of sand at 0.01 m compared to sand at 10 m, for which the spectra are all much closer together (especially as blue and red wavelengths) and thus have smaller covariances. The class covariance matrix defines the size of the "swarm of points" surrounding the centroid (mean class spectrum) representing the class in K-dimensional R_{rs} space. The image spectrum is assigned to a particular class according to a statistical model (often based on the assumption of a multivariate normal distribution of the swarm of points) that determines the probability that the image spectrum belongs to a particular the swarm of points defining a given class. The class spectra (K-dimensional swarms of points) generally overlap, so that an unambiguous, non-probabilistic association of $\boldsymbol{I}$ with a given class is not possible.

In maximum likelihood estimation (MLE; see Richards and Jia 1996 for an excellent discussion of this whole business), the distance metric is

$$D_{MLE}^2(m) = \ln|\boldsymbol{\Sigma}_m| + [\boldsymbol{I} - \bar{\boldsymbol{R}}_m]^T \boldsymbol{\Sigma}_m^{-1} [\boldsymbol{I} - \bar{\boldsymbol{R}}_m] ,$$

where $|\boldsymbol{\Sigma}_m|$ denotes the determinant of $\boldsymbol{\Sigma}_m$ and $\boldsymbol{\Sigma}_m^{-1}$ denotes the inverse. $|\boldsymbol{\Sigma}_m|$ and $\boldsymbol{\Sigma}_m^{-1}$ are of course pre-computed for each class before doing the spectrum matching. The image spectrum $\boldsymbol{I}$ is assigned to the class m having the smallest value of $D_{MLE}^2(m)$. This metric involves matrix multiplication, which is computationally expensive, but the number of classes is generally small, so in practice this may not be a problem.

It is often said that the incorporation of $\boldsymbol{\Sigma}_m$ into the distance metric "removes the effect of correlations between wavelengths." This interpretation of the effect of $\boldsymbol{\Sigma}_m$ relates to the fact that

covariance matrices are the foundation of principle component analysis (PCA; see Preisendorfer, 1988 for the definitive discussion of PCA). In PCA the original independent, physical variables (here, the wavelengths) are transformed to obtain a new set of (generally unphysical) independent variables for which the data are uncorrelated. This transformation can be viewed as a rotation of the axes of the original, physical data space (here the wavelength axes used for plots in K-dimensional space) to generate new (generally unphysical) axes for which the data are uncorrelated.

If the class covariances are equal (or assumed to be equal), then $\ln|\mathbf{\Sigma}_m|$ is the same for each class and can be ignored. The MLE metric then reduces to the Mahalanobis distance metric,

$$D_M^2(m) = [\boldsymbol{I} - \bar{\boldsymbol{R}}_m]^T \, \mathbf{\Sigma}^{-1} \, [\boldsymbol{I} - \bar{\boldsymbol{R}}_m] ,$$

where $\mathbf{\Sigma}$ is the common value of $\mathbf{\Sigma}_m$. The image spectrum $\boldsymbol{I}$ is then assigned to the class m having the smallest value of $D_M^2(m)$.

We have seen by the specific examples of Fig. A.2 and Table A.1 that the covariance matrices are different for different classes of the sort that are of interest for ocean remote sensing. Indeed, Table A.1 shows that the elements of the $\mathbf{\Sigma}_m$ can change by orders of magnitude as a function of water depth. This inequality of the $\mathbf{\Sigma}_m$ for different classes precludes use of the Mahalanobis metric for classes as defined here. For the retrievals addressed by CRISTAL, MLE (or something else) would have to be used with a different covariance matrix for each class.

However, it is not at all clear how meaningful classes should be defined for simultaneous retrievals of bottom type, water column IOPs, and bottom depth. Should one class be "sand spectra at 5.25 m depth with a particular set of water absorption, scattering, and backscatter spectra," and another class be "sand spectra at 5.25 m depth with the same absorption and scattering spectra but a different backscatter fraction," and another class be "sand spectra at 5.50 m with the first set of IOPs," and then another class be "sea grass spectra at 7.50 m with yet another set of IOPs," and so on? If so, then the number of classes quickly becomes as large as the number of depths, IOP sets, and pre-chosen classes of bottom type (sand, coral, grass, etc.). There could easily be several hundred classes (a CRISTAL database often has 50-100 bottom depths, several dozen to several hundred sets of IOPs, and ~100 bottom reflectance spectra). With such a large number of classes, the validity of doing traditional thematic mapping becomes uncertain, not to mention the additional computational costs involved with the matrix multiplications.

Clearly the CRISTAL technique addresses a much more complicated problem than classic thematic mapping, which corresponds to retrieval of bottom type if there were no water present—i.e., no simultaneous retrieval of depth and IOPs. Because of the greater complexity of the present retrieval problem, and because of the difficulty in defining meaningful classes, CRISTAL does not use statistical classification techniques such as MLE. CRISTAL does not compare an image spectrum to a class mean spectrum. CRISTAL compares an image spectrum to every spectrum in its database, and finds the closest match by the Euclidean (or some other) metric, which is

appropriate in this case. In a manner of speaking, each CRISTAL database R_{rs} spectrum is a separate class corresponding to a particular depth, bottom reflectance spectrum, and set of IOPs. In such a situation (only one member in each class) the covariance matrix is undefined.

Moreover, for the present problem it is not even desirable to remove the effects of wavelength correlations, as can be done with the MLE or Mahalanobis metrics, because the wavelength correlations carry information that is critical to separating depth and IOPs effects from bottom type effects.

The CRISTAL approach is therefore to avoid defining predetermined classes and to find the closest match from the entire database. This gives the highest possible resolution of retrievals. Thus for example, CRISTAL retrieves a particular bottom reflectance spectrum (which represents a particular bottom type), not just a generic bottom type such as sand or coral. If the user wishes to later group the particular spectra for the retrieved bottom types into broader classes such as corals vs. sediments, or to group the retrieved IOPs into low, medium, and high absorption bins, for example, then that is easily done from the full-resolution retrieval.

We have investigated numerous metrics for spectrum matching, include MLE and Mahalanobis metrics with various class definitions. The metrics that give best CRISTAL results are the Euclidean, Manhattan, and Correlation metrics discussed in Section 3.1.

In conclusion, **CRISTAL does not perform statistical classification in the usual sense, for good reason,** and the use if the Euclidean metric as the default for matching image and database spectra is well justified.